EPR-Based Trilateration

DOI: 10.1002/anie.201410396

EPR-Based Approach for the Localization of Paramagnetic Metal Ions in Biomolecules**

*Dinar Abdullin, Nicole Florin, Gregor Hagelueken, and Olav Schiemann**

Abstract: *Metal ions play an important role in the catalysis and folding of proteins and oligonucleotides. Their localization within the three-dimensional fold of such biomolecules is therefore an important goal in understanding structure–function relationships. A trilateration approach for the localization of metal ions by means of long-range distance measurements based on electron paramagnetic resonance (EPR) is introduced. The approach is tested on the Cu^{2+} center of azurin, and factors affecting the precision of the method are discussed.*

Metal ions are often crucial for the folding and structural integrity of biomolecules, and they are centers of catalysis in metalloproteins[1] and some ribozymes.[2] To understand how these biomolecules perform their function, it is important to know the location of the metal ions in the biomolecular structure. X-ray crystallography can provide this information with high precision. However, it is not always possible to grow crystals of a biomolecule, and in some cases only the metal-free structure can be crystallized. It is also not always possible to crystallize different conformational states of biomolecules that they adopt during folding or function. Another suitable method is high-resolution nuclear magnetic resonance (NMR) spectroscopy. It can be applied in solution and delivers the structure and dynamics of diamagnetic and paramagnetic biomolecules at an atomistic level, but is limited to biomolecules smaller than about 70 kDa.[3] If the metal ion to be localized is luminescent, also fluorescence resonance energy transfer (FRET) might be applied.[4] Nevertheless, there are still examples where the position of the metal ion in a biomolecule is not determined, for example, copper binding sites in amyloid precursor protein or manganese binding sites in ribozymes.[5] Therefore, complementary to these methods, we report herein a concept for the localization of paramagnetic metal ions by means of electron paramagnetic resonance (EPR) spectroscopy. EPR is very powerful in detecting and characterizing paramagnetic species including paramagnetic metal ions.[6] Compared to the methods above, EPR does not require crystallization of biomolecules, can be applied in solution, is not restricted by the biomolecular size and does not require a reference sample. The idea of the EPR-based approach is similar to the global positioning system (GPS) that can locate an object on the surface of the Earth by measuring distances to a number of GPS satellites: Here, the position of a metal ion in a biomolecular structure can be determined via distance constraints measured between this ion and a number of spin labels attached to the surface of the biomolecule by site-directed spin labelling.[7] The attached spin labels act as reference points in the molecular coordinate system of the biomolecule. Their approximate coordinates can be obtained from computational spin labeling programs, as for example, MMM,[8] mtsslWizard,[9] or PRONOX,[10] and the distance constraints can be measured by EPR techniques, which explore the dipolar interaction between pairs of electron spins.[11] The most common method for distance measurements in the range of 1.5–8 nm is pulsed electron–electron double resonance (PELDOR or DEER).[12]

Recently, a nitroxide-labeled lipid in soybean seed lipoxygenase-1 was localized by trilateration,[13] and two EPR-derived distance constraints were used to narrow down the location of a Cu^{2+} ion in the EcoRI endonuclease–DNA complex.[14] Yet, up until now the precision of the approach has not been tested, and there have been no reports on an EPR-based trilateration of a metal ion in a biomolecule. Metal ions introduce an additional complexity to the approach, because orientation selectivity of the PELDOR experiment and spin density delocalization may have to be taken into account. Therefore, we test in this work the EPR-based trilateration approach on the Cu^{2+} ion in the soluble blue copper protein azurin (Figure 1a). The results are compared with the crystallographic data and the precision of the method and factors influencing it are discussed.

To perform the trilateration, six single cysteine mutants of azurin were expressed, purified, and spin-labeled with (1-oxyl-2,2,5,5-tetramethylpyrroline-3-methyl)methanethiosulfonate (MTSSL): T21C, T30C, T61C, D69C, T96C, and S100C (Figure 1a; Supporting Information). All labeled mutants showed the expected blue color, symmetric gel-filtration peaks at elution volumes corresponding to monomeric azurin (Supporting Information, Figure S1) and continuous-wave X-band EPR spectra confirming the presence of only protein-bound MTSSL spin labels (Supporting Information, Figure S2).

The distance between the Cu^{2+} ion and MTSSL were measured for each of the six mutants by the four-pulse PELDOR technique (Supporting Information). To achieve a large modulation depth, the PELDOR experiments were

[*] D. Abdullin, N. Florin, Dr. G. Hagelueken, Prof. Dr. O. Schiemann
Institute of Physical and Theoretical Chemistry
University of Bonn
Wegelerstrasse 12, 53115 Bonn (Germany)
E-mail: schiemann@pc.uni-bonn.de
Homepage: http://www.schiemann.uni-bonn.de

[**] This work was funded by the German Research Foundation (DFG) with a grant for project A6 within the collaborative research centre SFB813 "Chemistry at Spin Centres".

Supporting information for this article is available on the WWW under http://dx.doi.org/10.1002/anie.201410396.

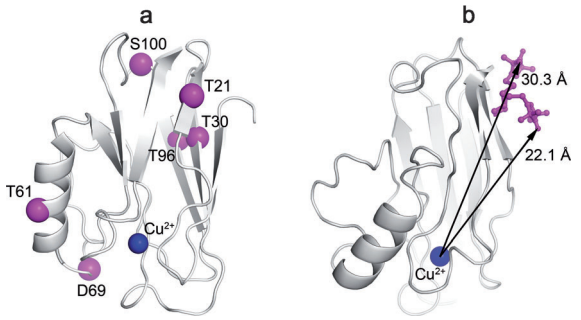

Figure 1. a) The structure of azurin (PDB 1E67) and the chosen mutation labeling sites (pink spheres). b) The crystal structure of the azurin mutant $T21R_1$ (PDB 4BWW) with the two different conformations of MTSSL overlaid.[15] The distance vectors connecting the Cu^{2+} ion with the oxygen atom of MTSSL in $T21R_1$ are shown by arrows.

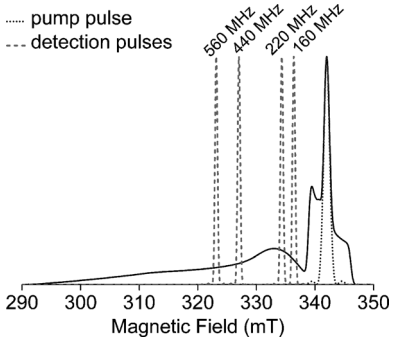

Figure 2. Hahn echo-detected field swept X-band EPR spectrum of azurin mutant $T21R_1$ shown together with the simulated excitation profiles of the 18 ns pump pulse and the 16–32 ns detection pulses.

performed by applying the pump pulse on the maximum of the nitroxide spectrum and the detection pulses at frequencies 160, 220, 440, and 560 MHz higher than the frequency of the pump pulse. Owing to the narrow excitation bandwidth of the pulses (Figure 2), the detection pulses select in dependence of the frequency-offset different spectral components of the copper spectrum and therefore different orientations of the dipolar distance vector connecting the copper ion with the nitroxide.[16] This orientation selection has to be taken into account in the analysis.

The background-subtracted PELDOR time traces of the six azurin mutants are compiled in Figure 3a. All of the time traces exhibit prominent dipolar oscillations and have modulation depths similar to the modulation depths observed for Cu^{2+}/nitroxide model systems.[16] The period of the oscillations and the modulation depth vary between the different frequency offsets, owing to the orientation selectivity and the limited bandwidth of the EPR resonator, which leads to longer pump pulses and therefore smaller modulation depths at larger offsets.

Owing to the orientation selectivity, distance distributions cannot be accurately extracted from a single PELDOR time trace. Therefore, we applied three alternative methods of data analysis. In the simplest method, the distances are estimated from the perpendicular component ($\nu_\perp$) of the Pake doublet, which is obtained after Fourier transformation (FFT) of the

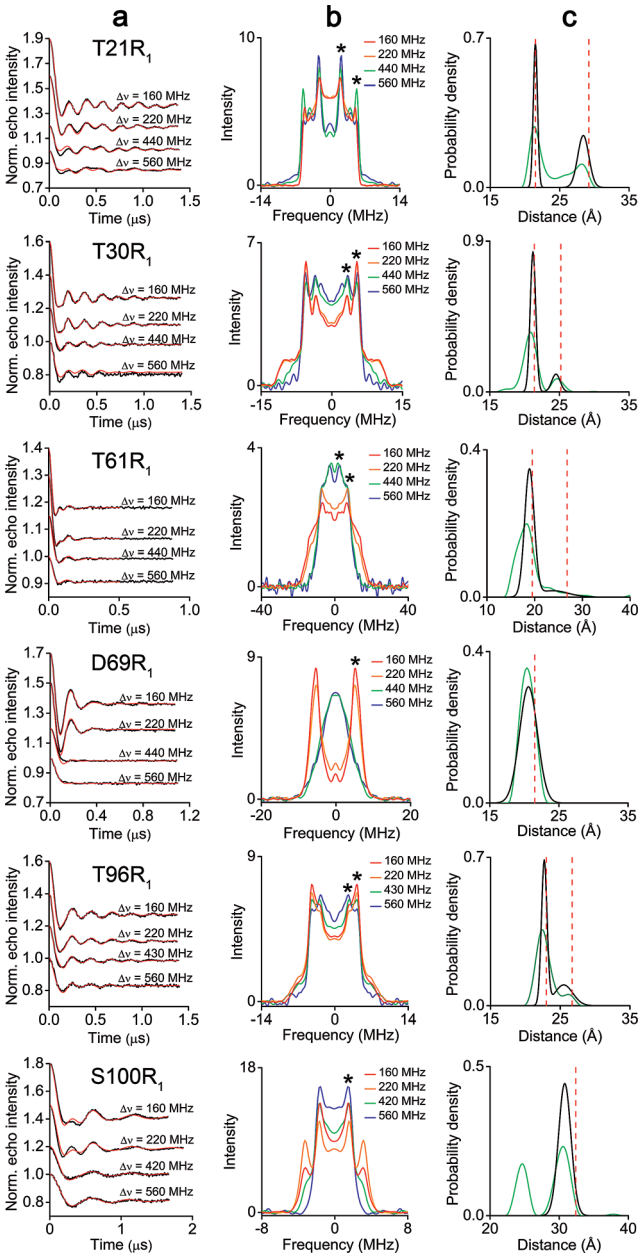

Figure 3. PELDOR data of the six azurin mutants. a) The background corrected PELDOR time traces (black) overlaid with their fits obtained from the PeldorFit program (red). b) The FFTs of the time traces. The positions of the $\nu_\perp$ frequencies are marked by asterisks. c) The distance distributions obtained with FFT (red dashed), DeerAnalysis (green), and PeldorFit (black).

PELDOR time traces and averaging over the four FFTs for each mutant (Figure 3b). In the second method, the time traces recorded with different frequency offsets are summed, again to reduce the orientation selectivity, and then analyzed by Tikhonov regularization as implemented in the DeerAnalysis program.[17] The accuracy of the distance distributions obtained by this approach depends on the efficiency of the orientation averaging. This efficiency is usually small for broad EPR spectra of metal ions. The third method uses the PeldorFit program,[18] which fits the four PELDOR time

Table 1: PELDOR-derived Cu^{2+}-MTSSL distances and their predictions from the molecular simulations.

Mutant	FFT [Å][a]	FFT, average [Å][a]	DeerAnalysis [Å][b]	DeerAnalysis, average [Å][b]	PeldorFit [Å][b]	PeldorFit, average [Å][b]	mtsslWizard [Å][c]
$T21R_1$[d]	21.5, 5.1; 29.2, 1.3	25.3, 3.7	21.7, 1.0; 27.3, 1.4	23.8, 2.9	21.5, 0.3; 28.4, 0.8	24.9, 3.5	24
$T30R_1$	21.4, 2.4; 25.2, 1.3	23.3, 1.9	20.6, 1.1; 24.8, 0.8	21.3, 1.9	21.2, 0.4; 24.5, 0.6	21.7, 1.3	25
$T61R_1$	19.5, 1.9; 26.8, 6.1	23.1, 4.5	18.0, 1.7; 25.3, 2.6	18.9, 3.2	18.9, 1.0; 23.8, 3.2	19.6, 2.3	21
$D69R_1$	21.5, 1.3	21.5, 1.3	20.5, 1.1	20.5, 1.1	20.6, 1.3	20.6, 1.3	20
$T96R_1$	23.0, 1.7; 26.7, 3.0	24.8, 2.4	22.6, 1.0; 26.1, 0.7	23.0, 1.5	22.7, 0.4; 25.5, 1.3	23.6, 1.5	24
$S100R_1$	32.4, 7.8	32.4, 7.8	30.4, 1.0	30.4, 1.0	30.8, 0.9	30.8, 0.9	33

[a] Distances are given in the form of mean value, error (for calculation of errors, see the Supporting Information). [b] Distances are given in the form of mean value, standard deviation. [c] Distances averaged over all generated MTSSL conformers are given. [d] Distances calculated from the crystal structure are 22.1 Å and 30.3 Å.

traces with one set of parameters and provides a geometric model of the spin pair, taking orientation selection into account (Supporting Information).

The distances obtained by these three methods are shown in Figure 3c and Table 1. Interestingly, bimodal distributions were found with all three methods for mutants $T21R_1$, $T30R_1$, $T61R_1$, and $T96R_1$. Since the wild-type azurin cannot be labeled to any significance (Supporting Information, Figure S2), a second labeling site as reason for the second distance can be excluded. At the same time, the pronounced bimodal distance distribution found for mutant $T21R_1$ fits to the crystal structure of this mutant, revealing the presence of two MTSSL conformations (Figure 1b).[15] Moreover, the Cu^{2+}–MTSSL distances calculated for these conformations are in very good agreement with the distances determined by PELDOR (Table 1). In the three other mutants, the second distance peak appears only as a shoulder, but also for these cases the presence of two MTSSL conformations is the most likely explanation. Note that the presence of distinct MTSSL conformations has been found also for other proteins.[19]

To convert the obtained distances into single-value distance constraints required for the trilateration, the corresponding mean distances and standard deviations were calculated (Table 1). Along with the distance constraints, the trilateration requires the coordinates of MTSSL within the molecular frame of azurin. As the reference coordinate system, the crystal structure of the metal-free (*apo*) form of azurin (PDB 1E65) is used. Models of MTSSL attached to the protein surface are created within this coordinate system by means of the program mtsslWizard (Supporting Information, Figure S8). Owing to the intrinsic flexibility of MTSSL, many conformers are created for each site. Therefore, to perform the trilateration, the coordinates of MTSSL at each individual site were averaged over all conformers.

Finally, the trilateration problem is solved by means of the program mtsslTrilaterate[20] using the distance constraints from PeldorFit and the MTSSL coordinates from mtsslWizard (Supporting Information). The position of the Cu^{2+} ion obtained from the calculations is shown within the azurin structure in Figure 4a. It is drawn as an ellipsoid with a center set to the most probable coordinates and semi-principal axes set to the doubled standard errors (2σ, 95% confidence level). To compare this solution with the crystallographic position of the Cu^{2+} ion, the structure of metal-bound azurin was superimposed onto the *apo* structure. The superposition

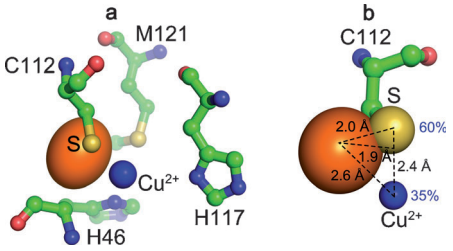

Figure 4. The trilateration of the Cu^{2+} ion in azurin overlaid with a) the crystallographic position of Cu^{2+} and b) its spin density distribution (the spin densities on the Cu and S atoms are shown in percent). The calculated 2σ area of the Cu^{2+} ion location is depicted by an orange ellipsoid, and the corresponding crystallographic position is shown by a blue sphere. The amino acid site chains comprising the binding site are shown as ball-and-stick models.

revealed high similarities between both structures (RMSD of 0.22 Å for 741 atoms), meaning that the binding site is preserved in both structures. As one can see from Figure 4a, the trilateration result places the Cu^{2+} ion within the binding site comprised of residues H46, H117, C112, and M121. Yet, a small shift of the calculated Cu^{2+} position from the corresponding crystallographic site towards the residue C112 is obtained. The value of this shift amounts to 2.6 Å and is the error of the trilateration result. However, it has to be kept in mind that PELDOR is sensitive to the spin density distribution and about 60% of the spin density is located on the sulfur atom of residue C112 and only 35% reside on the Cu^{2+} ion.[21] As a consequence, the obtained distances correspond to the distribution of the spin density, the midpoint of which is shifted from the Cu^{2+} ion towards the sulfur of C112 by 1.5 Å (Figure 4b). This explains the shift of the obtained solution towards residue C112. The offset between the center of the trilateration result and the weighted average position of the spin density is 1.9 Å. In principle, the spin-density distribution can be taken into account already at the stage of the distance calculation,[16b,c] but if the structure of the binding site is not known, this is not possible to achieve.

The remaining error arises from errors in the distance constraints and the MTSSL coordinates. As the exact values of the distances and coordinates are unknown, these errors cannot be easily quantified and separated from each other. Nevertheless, to estimate the error of the MTSSL coordinates, the experimental distances obtained from the PeldorFit

analysis were compared to the corresponding values predicted by mtsslWizard for the crystal structure of metal-bound azurin (Table 1). This comparison revealed an average deviation of 1.5 Å, which is in the same range as found in benchmark studies of the computational spin-labelling programs.[8,9] The error of the PeldorFit analysis is below 1 Å for the distances corresponding to the prominently populated MTSSL conformer, but can increase up to 3 Å for the weakly populated conformer (Supporting Information, Table S3). Furthermore, to estimate the error that the different PELDOR data analysis methods introduce into the distance constraints, the trilateration was performed alternately with distances obtained from the three different methods outlined above (Table 1). Using DeerAnalysis yields a solution deviating by 2.7 Å from the Cu^{2+} crystallographic site and thus having a similar precision as the solution found for the PeldorFit-derived distances. With the distances derived from the FFT approach, this difference increases up to 4.2 Å (Supporting Information, Figure S9). This result shows the importance of an accurate PELDOR data analysis.

Another parameter that influences the precision of trilateration is the number of spin label sites/distance constraints. To reveal this dependence, the trilateration was performed for 6, 5, and 4 constraints (Supporting Information, Figure S10). The results of the experiment show a gradual decrease of the error for the calculated Cu^{2+} position from 4.4 Å for 4 constraints down to 2.6 Å for 6 constraints. Moreover, the average 2σ of the calculated Cu^{2+} coordinates decreases from 2.9 Å down to 1.7 Å, and thus rendering the solution more localized. As a result, increasing the number of constraints improves the precision of trilateration, but requires longer experimental time. Beyond the number of used spin labels, their position with respect to the metal binding site and with respect to each other also affects the result of trilateration. The most reliable solution is achieved when all spin labels are evenly distributed on the protein surface.

Furthermore, the quality of the protein structure or its model has an impact on the trilateration result. To test this, we created a homology model of azurin using the structure of the related blue copper protein auracyanin as starting structure (PDB 2AAN, 30% identical amino acids, RMSD of 1.26 Å between both structures) for the SWISS-MODEL server[22] (Supporting Information). This test revealed that the calculated position of the Cu^{2+} ion is again very close to the binding site (error of 2.0 Å, $2\sigma = 1.6$ Å; Supporting Information, Figure S11) and shows that minor imperfections in the model structure are tolerated.

In conclusion, the EPR-based trilateration approach for metal ions in biomolecules has been successfully tested for the Cu^{2+} center in azurin. The calculated position of the Cu^{2+} ion is within the metal binding site and has a difference to the corresponding crystallographic position of 2.6 Å. The obtained precision of the method is affected by the spin density distribution of the metal center, the accuracy of the MTSSL models, and the number and position of the distance constrains. The error related to the spin density distribution might be further reduced by combining the trilateration approach with electron nuclear double-resonance experiments. This approach can be transferred to other metal ions, including high-spin metal ions such as Fe^{3+} or Mn^{2}. It can be also useful for correlating the position of metal ions found by X-ray crystallography with EPR spectroscopically identified metal ions.[5b] And last but not least, it can be applied for localizing metal ions in folding intermediates or in conformational states of biomolecules. In these cases, models of the biomolecular structure, perhaps constraint by nitroxide–nitroxide distance measurements, would be a prerequisite.

Received: October 23, 2014
Published online: December 17, 2014

Keywords: binding sites · copper · EPR spectroscopy · spin labels · triangulation

[1] *Handbook of Metalloproteins*, *Vol. 4–5* (Ed.: J. Finkelstein), Wiley, Chichester, **2011**.
[2] *Ribozymes and RNA Catalysis* (Eds.: D. M. J. Lilley, F. Eckstein), RSC, Cambridge, **2008**.
[3] a) A. M. J. J. Bonvin, R. Boelens, R. Kaptein, *Curr. Opin. Chem. Biol.* **2005**, *9*, 501–508; b) I. Bertini, C. Luchinat, G. Parigi, R. Pierattelli, *Dalton Trans.* **2008**, 3782–3790.
[4] a) A. Muschielok, J. Andrecka, A. Jawhari, F. Bruckner, P. Cramer, J. Michaelis, *Nat. Methods* **2008**, *5*, 965–971; b) J. W. Taraska, M. C. Puljung, W. N. Zagotta, *Proc. Natl. Acad. Sci. USA* **2009**, *106*, 16227–16232.
[5] a) K. J. Barnham, W. J. McKinstry, G. Multhaup, D. Galatis, C. J. Morton, C. C. Curtain, N. A. Williamson, A. R. White, M. G. Hinds, R. S. Norton, K. Beyreuther, C. L. Masters, M. W. Parker, R. Cappai, *J. Biol. Chem.* **2003**, *278*, 17401–17407; b) N. Kisseleva, S. Kraut, A. Jäschke, O. Schiemann, *HFSP J.* **2007**, *1*, 127–136.
[6] a) *Paramagnetic Resonance of Metallbiomolecules* (Ed.: J. Telser), American Chemical Society, Washington, DC, **2003**; b) S. van Doorslaer in *Electron Paramagnetic Resonance*, *Vol. 21* (Ed.: B. C. Gilbert), RSC, London, **2008**, pp. 162–183; c) D. Goldfarb in *Structure and Bonding*, *Vol. 152* (Eds.: C. R. Timmel, J. R. Harmer), Springer, Berlin/Heidelberg, **2014**, pp. 163–204.
[7] a) C. Altenbach, T. Marti, H. Khorana, W. Hubbell, *Science* **1990**, *248*, 1088–1092.
[8] Y. Polyhach, E. Bordignon, G. Jeschke, *Phys. Chem. Chem. Phys.* **2011**, *13*, 2356–2366.
[9] G. Hagelueken, R. Ward, J. Naismith, O. Schiemann, *Appl. Magn. Reson.* **2012**, *42*, 377–391.
[10] M. M. Hatmal, Y. Li, B. G. Hegde, P. B. Hegde, C. C. Jao, R. Langen, I. S. Haworth, *Biopolymers* **2012**, *97*, 35–44.
[11] a) O. Schiemann, T. F. Prisner, *Q. Rev. Biophys.* **2007**, *40*, 1–53; b) G. Jeschke, *Annu. Rev. Phys. Chem.* **2012**, *63*, 419–446; c) P. P. Borbat, J. H. Freed in *Structure and Bonding*, *Vol. 152* (Eds.: C. R. Timmel, J. R. Harmer), Springer, Berlin/Heidelberg, **2014**, pp. 1–82.
[12] a) A. D. Milov, K. M. Salikhov, M. D. Shirov, *Fiz. Tverd. Tela* **1981**, *23*, 975–982; b) R. E. Martin, M. Pannier, F. Diederich, V. Gramlich, M. Hubrich, H. W. Spiess, *Angew. Chem. Int. Ed.* **1998**, *37*, 2833–2837; *Angew. Chem.* **1998**, *110*, 2993–2998.
[13] B. J. Gaffney, M. D. Bradshaw, S. D. Frausto, F. Wu, J. H. Freed, P. Borbat, *Biophys. J.* **2012**, *103*, 2134–2144.
[14] Z. Yang, M. R. Kurpiewski, M. Ji, J. E. Townsend, P. Mehta, L. Jen-Jacobson, S. Saxena, *Proc. Natl. Acad. Sci. USA* **2012**, *109*, E993–E1000.
[15] N. Florin, O. Schiemann, G. Hagelueken, *BMC Struct. Biol.* **2014**, *14*, 16.

[16] a) E. Narr, A. Godt, G. Jeschke, *Angew. Chem. Int. Ed.* **2002**, *41*, 3907 – 3910; *Angew. Chem.* **2002**, *114*, 4063 – 4066; b) B. E. Bode, J. Plackmeyer, T. F. Prisner, O. Schiemann, *J. Phys. Chem. A* **2008**, *112*, 5064 – 5073; c) B. E. Bode, J. Plackmeyer, M. Bolte, T. F. Prisner, O. Schiemann, *J. Organomet. Chem.* **2009**, *694*, 1172 – 1179; d) J. Sarver, K. I. Silva, S. Saxena, *Appl. Magn. Reson.* **2013**, *44*, 583 – 594.

[17] a) G. Jeschke, V. Chechik, P. Ionita, A. Godt, H. Zimmermann, J. Banham, C. R. Timmel, D. Hilger, H. Jung, *Appl. Magn. Reson.* **2006**, *30*, 473 – 498; b) A. Godt, M. Schulte, H. Zimmermann, G. Jeschke, *Angew. Chem. Int. Ed.* **2006**, *45*, 7560 – 7564; *Angew. Chem.* **2006**, *118*, 7722 – 7726.

[18] D. Abdullin, G. Hagelueken, R. I. Hunter, G. M. Smith, O. Schiemann, *Mol. Phys.* DOI: 10.1080/00268976.2014.960494.

[19] a) G. Hagelueken, W. J. Ingledew, H. Huang, B. Petrovic-Stojanovska, C. Whitfield, H. ElMkami, O. Schiemann, J. H. Naismith, *Angew. Chem. Int. Ed.* **2009**, *48*, 2904 – 2906; *Angew. Chem.* **2009**, *121*, 2948 – 2950; b) C. J. López, Z. Yang, C. Altenbach, W. L. Hubbell, *Proc. Natl. Acad. Sci. USA* **2013**, *110*, E4306 – E4315.

[20] G. Hagelueken, D. Abdullin, R. Ward, O. Schiemann, *Mol. Phys.* **2013**, *111*, 2757 – 2766.

[21] a) M. van Gastel, J. W. A. Coremans, H. Sommerdijk, M. C. van Hemert, E. J. J. Groenen, *J. Am. Chem. Soc.* **2002**, *124*, 2035 – 2041; b) C. Remenyi, R. Reviakine, M. Kaupp, *J. Phys. Chem. B* **2007**, *111*, 8290 – 8304.

[22] K. Arnold, L. Bordoli, J. Kopp, T. Schwede, *Bioinformatics* **2006**, *22*, 195 – 201.

